

The Galactic Center: An Interacting System of Unusual Sources

F. Yusef-Zadeh,¹ F. Melia,² M. Wardle³

The region bounded by the inner tens of light-years at the center of the Milky Way Galaxy contains five principal components that coexist within the central deep well of gravitational potential. These constituents are a black hole candidate (Sgr A*) with a mass equivalent to $2.6 \pm 0.2 \times 10^6$ solar masses, a surrounding cluster of evolved stars, a complex of young stars, molecular and ionized gas clouds, and a powerful supernova-like remnant. The interaction of these components is responsible for many of the phenomena occurring in this complex and unique portion of the Galaxy. Developing a consistent picture of the primary interactions between the components at the Galactic center will improve our understanding of the nature of galactic nuclei in general, and will provide us with a better-defined set of characteristics of black holes. For example, the accretion of stellar winds by Sgr A* appears to produce far less radiation than indicated by estimates based on models of galactic nuclei.

Sgr A* is a bright, compact radio source at the dynamical center of the Galaxy, which was discovered 25 years ago (1). This object is a very strong candidate for a massive black hole and is the anchor about which stars and gas in its vicinity orbit. Sgr A* is embedded within two clusters of massive and evolved stellar systems orbiting with increasing velocity dispersion toward it, based on stellar radial velocity measurements (2–5) providing a measure of the gravitational potential of the central mass. Based on a remarkable set of stellar proper motion data acquired over 6 years measuring the motion of stars down to a field as small as 5 light days from Sgr A*, a central concentration of dark mass of $2.6 \pm 0.2 \times 10^6$ solar masses (M_{\odot}) (6–9) has been found to lie within the inner 0.015 pc of the Galactic center. [0.1" corresponds to 800 astronomical units (AU) is defined as the average distance between Earth and the sun), or 1.2×10^{16} cm, or about 4.6 light days, or about 4×10^{-3} pc at the Galactic center distance assumed to be 8 kpc away from the sun.] The inferred distribution of matter as a function of distance from Sgr A* (Fig. 1) (10) and the stellar velocity dispersion measurements are consistent with Keplerian motion (Fig. 2) (11). The stellar kinematics within ~ 0.01 pc (3×10^{16} cm) of the Galactic center are dominated by underluminous matter, probably a massive black hole, and this is arguably the most accurate determination of the presence of dark matter within the nuclei

of galaxies, except perhaps for NGC 4258 (12).

However, showing that the Galactic center must contain a centralized mass concentration does not require that this dark matter be in the form of a compact object with a few million solar masses [as (13) had predicted]. It does not even imply that the unusual radio source Sgr A* must be associated with it, but it is possible to demonstrate that Sgr A* is probably not stellar. This is based on the fact that a heavy object in dynamical equilibrium with the surrounding stellar cluster will move slowly, so that a failure to detect proper motion in Sgr A* may be used to provide an independent estimate of its mass. In fact, such measurements have been carried out using the Very Large Array (VLA) of radio telescopes for about 17 years (14). More recently, similar measurements using the

Very Long Baseline Array (VLBA) derived a lower mass limit of $\sim 1000 M_{\odot}$, which appears to rule out the possibility that Sgr A* is a pulsar, a stellar binary, or a similarly small object (15).

Still, VLBA images of Sgr A* with milliarcsecond (mas) resolution (16) show that at a wavelength λ of 7 mm, its radius is 0.76 ± 0.04 mas, or roughly 6.2×10^{13} cm (about 4 AU), which is much smaller than the present limiting region within which the $2.6 \times 10^6 M_{\odot}$ are contained. So the dark matter may be distributed, perhaps in the form of white dwarfs, neutron stars, or black holes of $\sim 10 M_{\odot}$ (5). However, the latest stellar kinematic results appear to rule out the first two possible constituents. Genzel *et al.* (6) argue that a distribution of neutron stars in equilibrium with the central gravitational potential should have a core radius somewhere between 0.15 and 0.3 pc, which is larger than the value of ≤ 0.07 pc derived from the velocity data. The same holds true for a population of white dwarfs. Moreover, the neutron stars would presumably have been formed with a substantial "kick" and may not remain bound to the nucleus. Thus, as long as the dark matter distribution is in equilibrium, the only viable alternative to the massive black hole paradigm may be a distributed population of $\sim 10 M_{\odot}$ black holes. Whether such a concentration is stable against mergers that would eventually produce a single massive object is still an open question, although Maoz (17) has argued that the density of dark matter in

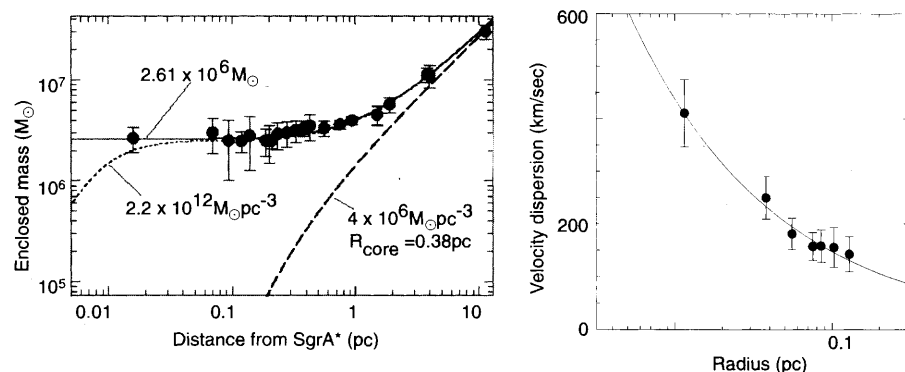


Fig. 1 (left). A plot of the distribution of enclosed mass versus distance from Sgr A*. The three curves represent the mass model for a nearly isothermal stellar cluster with a core radius of 0.38 pc (thick dashed line), the sum of this cluster plus a point mass of $2.61 \pm 0.35 \times 10^6 M_{\odot}$ (thin solid curve), the same cluster and a dark cluster with a central density of $2.2 \times 10^{12} M_{\odot} \text{pc}^{-3}$ and a core radius of 0.0065 pc (thin dotted curve) (10). Data were obtained with the New Technology Telescope (NTT). **Fig. 2 (right).** The projected stellar velocity dispersion versus the distance from Sgr A*. The solid curve represents Keplerian motion due to a mass concentrated within 0.01 pc (11). Data were obtained with the Keck telescope (NTT).

¹Department of Physics and Astronomy, Northwestern University, Evanston, IL 60208, USA. E-mail: zadeh@nwu.edu. ²Department of Physics and Steward Observatory, The University of Arizona, Tucson, AZ 85721, USA. E-mail: melia@as.arizona.edu. ³Special Research Centre for Theoretical Astrophysics, University of Sydney, Sydney, New South Wales 2006, Australia. E-mail: wardle@physics.usyd.edu.au

the Galactic center is so high ($>10^{12} M_{\odot} \text{pc}^{-3}$) that its lifetime as a stable cluster could not exceed $\sim 10^8$ years, which is much less than the age of the Galaxy.

The presence of dark matter centered on Sgr A* links the Galactic center to the broader class of active galactic nuclei (AGNs), in which a massive black hole is thought to dominate the dynamics and energetics of the nuclear region. A second fascinating characteristic of our Galaxy that it shares with AGNs is the existence of fragile molecules in a ring of neutral gaseous material orbiting only a few parsecs from the center, not unlike the parsec-sized obscuring tori invoked to explain some features of AGNs (18). The picture that has emerged from a suite of multiwavelength observations is that this molecular ring [also known as the circumnuclear disk (CND)], with a mass of $>10^4 M_{\odot}$, is clumpy and is rotating around a concentrated

cluster of hot stars (called IRS 16) with a velocity of about 110 km s^{-1} (Fig. 3A) (19–21). Most of the far-infrared (IR) luminosity of the CND can be accounted for by this cluster of hot, helium emission-line stars (22). The IRS 16 complex consists of about two dozen blue stellar components at $2 \mu\text{m}$ and appears to be the source of a strong wind with velocity on the order of 700 km s^{-1} and an inferred mass loss rate of $4 \times 10^{-3} M_{\odot} \text{ year}^{-1}$ (23–25). These blue stellar sources are themselves embedded within a cluster of evolved and cool stars with a radial density distribution r^{-2} from the dynamical center of the Galaxy. Unlike the distribution of the evolved cluster members, which extend over the central 500 pc of the Galactic bulge, the hot stars of the IRS 16 complex are concentrated within the inner parsecs of the Galaxy.

Within the cavity of molecular gas in the CND lies the ionized gas known as Sagittar-

ius A West (Sgr A West), which appears as a three-armed spiral-like structure (with north, east, and west arms) orbiting about Sgr A*, the IRS 16 cluster, and the peak of the distribution of evolved stars (Fig. 3A). The kinematics of ionized gas surrounding Sgr A* show systematic velocities along various components of Sgr A West ($\approx 30''$ west of Sgr A*) with a radial velocity structure that varies regularly between -100 and $+100 \text{ km s}^{-1}$ in the south-north direction (26–31). The velocity within the inner $10''$, where there is a hole in the distribution of ionized gas, known as the mini-cavity, becomes increasingly more negative down to $\approx -350 \text{ km s}^{-1}$ toward Sgr A* (32–33). These studies of gas motion over the past 20 years have consistently indicated the presence of a large concentration of mass at the Galactic center.

Whereas the stars orbit randomly around the Galactic center, the ionized gas is part of

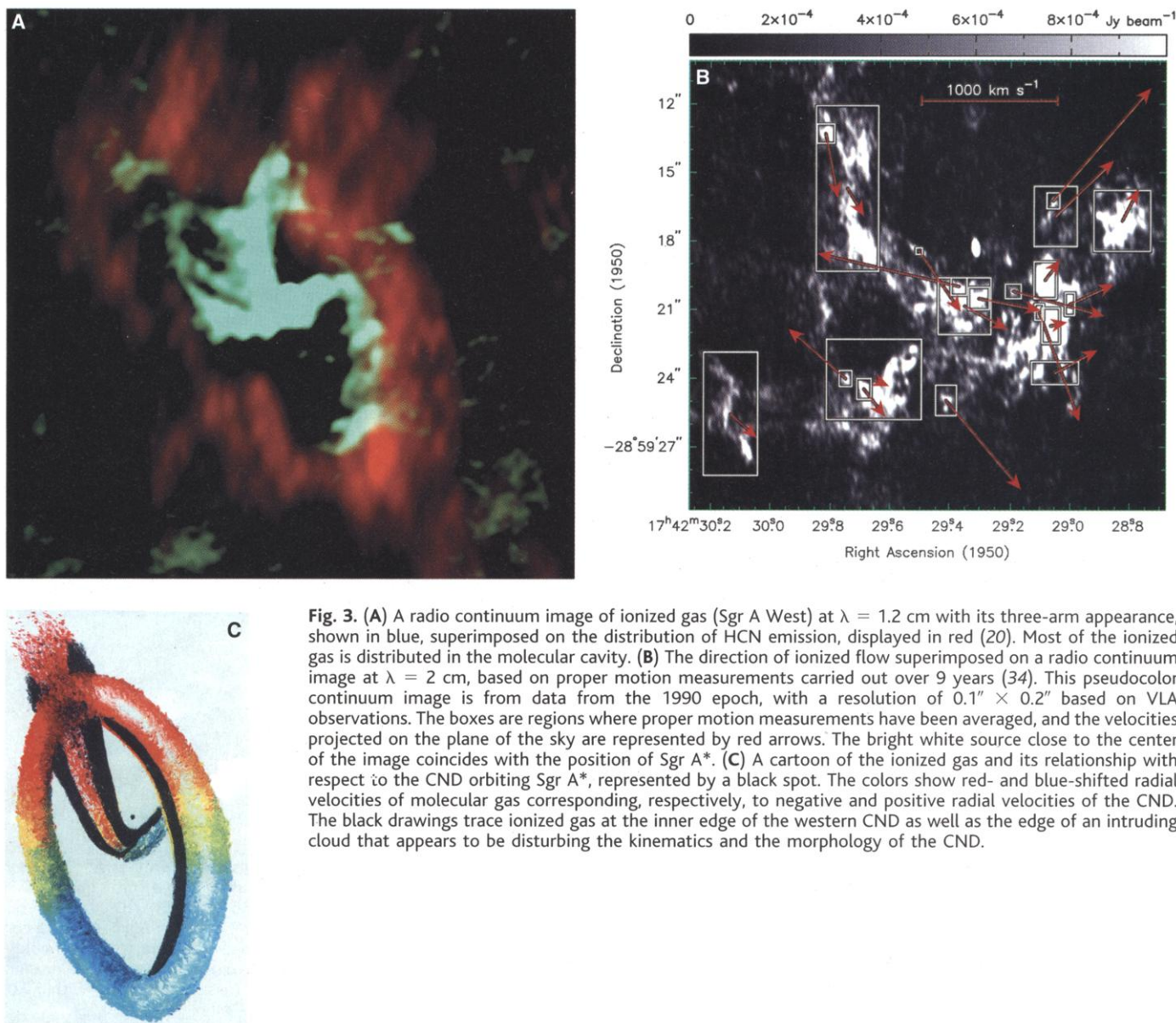


Fig. 3. (A) A radio continuum image of ionized gas (Sgr A West) at $\lambda = 1.2 \text{ cm}$ with its three-arm appearance, shown in blue, superimposed on the distribution of HCN emission, displayed in red (20). Most of the ionized gas is distributed in the molecular cavity. (B) The direction of ionized flow superimposed on a radio continuum image at $\lambda = 2 \text{ cm}$, based on proper motion measurements carried out over 9 years (34). This pseudocolor continuum image is from data from the 1990 epoch, with a resolution of $0.1'' \times 0.2''$ based on VLA observations. The boxes are regions where proper motion measurements have been averaged, and the velocities projected on the plane of the sky are represented by red arrows. The bright white source close to the center of the image coincides with the position of Sgr A*. (C) A cartoon of the ionized gas and its relationship with respect to the CND orbiting Sgr A*, represented by a black spot. The colors show red- and blue-shifted radial velocities of molecular gas corresponding, respectively, to negative and positive radial velocities of the CND. The black drawings trace ionized gas at the inner edge of the western CND as well as the edge of an intruding cloud that appears to be disturbing the kinematics and the morphology of the CND.

a coherent flow with a systematic motion that is decoupled from the stellar orbits. Understanding the kinematics of the system of ionized gas is complicated by our incomplete view of its three-dimensional geometry with respect to Sgr A* and is made more difficult by the interaction of the orbiting gas with nongravitational forces due to collisions with the winds produced by the central cluster of hot, mass-losing stars. Recently, the gas kinematics and the geometry of the ionized flow were determined by combining the transverse velocities measured over 9 years (Fig. 3B) and the radial velocities of ionized gas (34). In the region within the central 10" of Sgr A*, similar proper motion results have also been shown (35). The predominant component of the motion in the plane of the sky is from east to west for many of the features, with the exception of a few where the velocity of ionized gas is anomalously large, possibly the result of the interaction between the orbiting ionized gas and ionized stellar winds. It appears that the overall flow of ionized gas in the northern arm originates in the northeast with negative velocities in the orbital plane. The ionized gas follows an orbital trajectory to the southwest as it crosses a disturbed region of the CND and passes behind Sgr A* before it moves to the northwest (21, 36) (Fig. 3C). The strong gravitational potential due to the large concentration of dark matter near Sgr A* is responsible for velocity gradients exceeding $600 \text{ km s}^{-1} \text{ pc}^{-1}$.

Moving out from the Galactic center, to a scale of 10 to 20 pc, radio continuum observations show a prominent, nonthermal, continuum shell-like structure, known as Sgr A East. This extended source is superimposed onto the thermal source Sgr A West and the CND (Fig. 4). Low-frequency continuum observations show a decrease in the brightness of the Sgr A East shell at the position of Sgr A West, which results from free-free absorption (involves a change in the motion of the electron from one unbound orbit to another) of the radiation from the former by thermal gas in the latter. A good portion of Sgr A East must therefore lie behind Sgr A West (37–39).

Sgr A*: Colliding Winds and Their Interaction with the Black Hole

The highly compact nature of the distributed dark mass seems to suggest that we are dealing with a pointlike object. The gravitational field associated with such a source intensifies rapidly with decreasing distance to the origin, providing the necessary energy and confining power to stress any infalling gas to temperatures in excess of a billion degrees, which may explain the emissivity that produces the radiation we see from Sgr A*. However, suppose we play the Devil's advocate and consider the pos-

sibility that the dark matter is not in the form of a single massive black hole. In that case, whatever the composition of the distributed dark mass concentration is, one would be left with the daunting task of accounting for the nature of Sgr A* itself, without the benefit of invoking the deep well of gravitational potential of a pointlike object (40). Recently, Melia *et al.* (41) showed that a distribution of dark matter, even in the form of $\sim 10 M_{\odot}$ black holes, simply could not reproduce the spectrum of Sgr A*, because the gas in this region could not be squeezed to sufficiently high densities and temperatures to produce the observed radiative emission. However, a black hole exerts a stress on its nearby environment, which contains, in addition to the large-scale gaseous features described above, rather strong winds in and around Sgr A* itself. The close proximity of the heavy mass-losing stars of IRS 16 leads inevitably to frequent collisions between their winds, which results in a tessellation of broken flow segments when viewed from our perspective. This process not only disrupts the spherical winds from these stars, but (very important as far as the black hole is concerned) it facilitates the capture of gas by this object by reducing the plasma's kinetic energy and thereby curtailing its ability to escape from the strong gravitational field.

The portion of this wind plasma captured by the black hole falls inward toward the center with increasing speed as it approaches the event horizon. In the more energetic cores of distant galaxies, the outward push from the escaping radiation can decelerate the flow; this is not so in the Galactic center. Sgr A* does not radiate at a level sufficient to drive this infalling gas away, and the end result is that virtually all of the plasma within a tenth of a light-year or so is funneled into the black hole. Observationally, the key issue is why the infalling gas maintains a low radiative efficiency. If we naively take the calculated accretion rate onto the black hole and estimate the radiative power produced by the ensuing release of gravitational energy (42), we infer a total luminosity in excess of what is actually measured for Sgr A*. In fact, some estimates have it at 10^4 or 10^5 times the actual observed power.

The observations do not yet provide sufficient information for us to identify the physics of accretion when the infalling gas penetrates to within about 10^3 or 10^4 Schwarzschild radii of the central object (no light can escape when it has crossed the Schwarzschild radius of a black hole). The captured plasma is magnetized and highly ionized, but it is not clear how much specific angular momentum it carries, what the intensity of the magnetic field is, what the

relative importance of nonthermal and thermal particles is, and whether the plasma separates into a two-temperature fluid. As a result, a variety of assumptions are possible (and consistent with the observations), which results in a range of different interpretations. Beckert *et al.* (43) suggest that the radiation from Sgr A* results from shock waves in the accreting plasma, which produce a power-law electron energy distribution that is truncated by strong cooling. This forms a "quasi"-mono-energetic distribution. The overall emission, which is strictly nonthermal, is suppressed by constraining the number density of relativistic particles and the intensity of the magnetic field (at about 5 to 10 G). Falcke *et al.* (44), on the other hand, assume that the infalling plasma eventually produces a jet of power-law electrons whose number density varies with radius in the expulsion. The overall emission, which is a sum of nonthermal components, is also suppressed by constraining the particle number density and hence the equipartition magnetic field, both of which are assumed to be scaled by a slowly accreting fossilized disk. In a model developed by Narayan *et al.* (45, 46), the infalling gas carries more angular momentum, and a disk forms with an outer radius of about 10^5 Schwarzschild radii. Emission associated with the dissipation of the additional angular momentum is suppressed if the electron temperature (T_e) is much lower than that of the protons (T_p) ($T_e \ll T_p$), because it is the electrons that do the radiating.

One reason why the emissivity of Sgr A* is so low is that the magnetic field in the captured plasma is below its equipartition

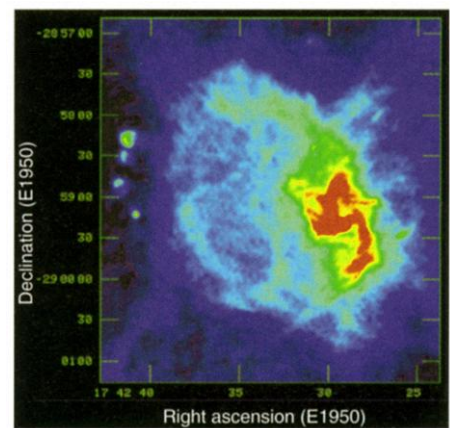


Fig. 4. VLA radio continuum image of the Galactic center showing the shell-like structure of nonthermal Sgr A East (light blue and green) and the spiral-shaped structure of thermal Sgr A West (red) at $\lambda = 6 \text{ cm}$ with a resolution of $3.4 \times 2.9 \text{ arc sec}$. A cluster of HII regions associated with Sgr A East is also evident to the east of the shell. The weak extended features (dark blue) surrounding the shell are part of the Sgr A East halo.

value. To address this problem, Kowalenko *et al.* (47) have begun to study the behavior of such a field as the ionized gas within which it is contained is compressed. They find that whereas the rate of increase in the magnetic field intensity due to flux conservation depends only on the rate of compression of the gas, the dissipation rate is a function of the state variables and is therefore not necessarily correlated with the simple equipartition of energy. The magnetic field remains subequipartition for most of the inflow, increasing rapidly only as the gas accelerates rapidly toward the event horizon, where the physical conditions (such as temperature and density) change more precipitously.

The emission in Sgr A* requires a very deep potential well, so the case for a massive black hole rather than distributed dark matter has grown stronger. Whether the radiation mechanism is thermal or nonthermal, the radiative efficiency of the infalling gas appears to be very low ($<10^{-5}$). All things considered, this low efficiency is probably due to either a subequipartition magnetic field (for either thermal or nonthermal models) or to the separation of the gas into a two-temperature plasma with $T_e \ll T_p$.

It is important to note, however, that only a fraction of the gas available from the stellar winds of IRS 16 is actually captured by the black hole and eventually accretes toward it. Much of the plasma is gravitationally focused as it passes by the central potential well, but remains unbound and continues to flow beyond the interaction zone, possibly affecting other gaseous structures in that region. Some evidence for this is provided by the presence of a chain of plasma blobs (Fig. 5A) that appear to be in transit from Sgr A* toward the ionized bar (Fig. 5B) located southwest of the dynamical center of the Galaxy (48–50). A small cavity (Fig. 5) has been carved out of the ionized bar (51, 52), possibly due to the impact of the collimated flow from the direction of the black hole. Indeed, hydrodynamical simulations suggest that the Bondi-Hoyle process responsible for the ac-

cretion of $\sim 10^{22} \text{ g s}^{-1}$ by Sgr A* also produces a downstream focused flow with a radius very similar to that of the cavity and a mechanical luminosity sufficient to power its radiative emission (51).

The Cometary Tail of IRS 7: A Supergiant Star Bathed by the Radiation and Winds from IRS 16

The IR source IRS 7 is a class M2I red supergiant lying within the projected distance of one light-year from the Galactic center (53, 54). This source, which is a member of the evolved cluster of stars, has a mass-losing envelope that is being ionized externally by the bath of ultraviolet (UV) radiation filling the central cavity (3, 32). Radio continuum observations have revealed a “cometary tail” of ionized gas from IRS 7 projected away from the dynamical center of the Galaxy (55). The kinematics of Ne^+ emission from IRS 7’s tail show conclusively that this ionized feature is physically associated with IRS 7 (56). Recently, Keck observations have shown that near-IR emission from the tail of IRS 7 has a dust temperature of $<200 \text{ K}$ (57). The detected free-free emission from the outer envelope of IRS 7 (Fig. 6) is consistent with photoionization by a UV radiation field of the strength inferred to lie within the inner 2 pc of the Galaxy (3, 32, 55, 56, 58), which implies a centrally concentrated source producing ionizing photons at a rate of $2 \times 10^{50} \text{ s}^{-1}$ (59–61).

These radio and mid-IR observations suggest that the observed phenomena may be explained by the ionization and subsequent removal of the mass-losing envelope of IRS 7 by the ram pressure associated with the nuclear wind. In this picture of the interaction between the evolved and young clusters, the ram pressure due to a pointlike Galactic center wind is responsible for ablating the circumstellar envelope of IRS 7. The tail, however, is longer and thinner than expected (Fig. 6) if the expanding stellar envelope is uniform. If this were actually the case, the radius of the head of IRS 7 would be determined by the standoff distance at which the ram pressures of the expanding envelope and the IRS

16 wind are comparable. The opening angle of the tail would be larger than observed, because the effective pressure of the wind acts only in the wind direction and cannot effectively confine the envelope perpendicular to the tail. Instead, the expanding envelope of IRS 7 is probably inhomogeneous (62, 63), as appears to be the case in other circumstellar envelopes. The stellar envelope then consists of a collection of clumps of dense gas moving radially outward from the central star. The inertia of the clumps is sufficient that their motion is unaffected by the drag from the nuclear wind, which slowly ablates material from their surfaces. The size of the head of the cometlike structure is then determined by the expansion speed of the envelope and the time scale for an individual clump to be ablated away. The thin tail is

Fig. 5. (Left) A VLA radio continuum image of the inner $20''$ of the Galactic center at $\lambda = 1.2 \text{ cm}$, with a resolution of $0.5'' \times 0.3''$, is displayed in blue and is superimposed on stellar distribution at $\lambda = 2 \mu\text{m}$ (95), displayed in red and white with a cell size of 50 mas. (Right) A schematic diagram showing major stellar and gaseous components of the Galactic center.

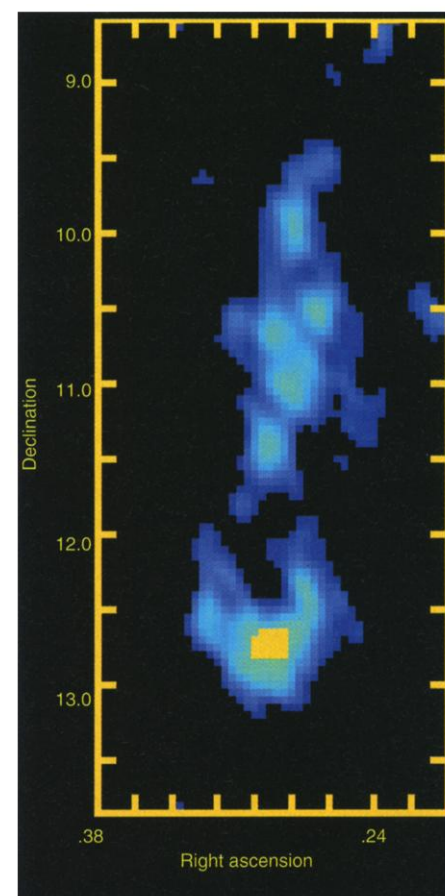
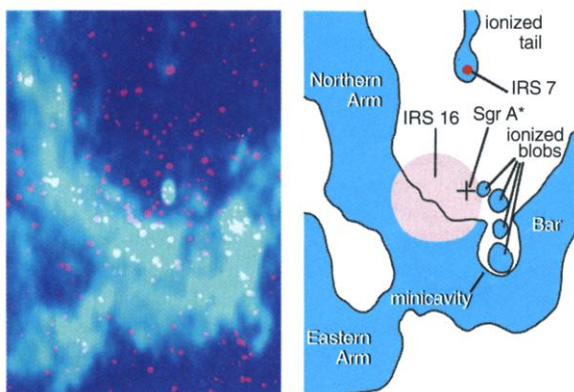


Fig. 6. The bow shock structure and the ionized tail of a cometary feature associated with IRS 7 at $\lambda = 1.2 \text{ cm}$ (blue), with a resolution of $0.3 \text{ arc sec} \times 0.2 \text{ arc sec}$, is superimposed on stellar emission from the photosphere of IRS 7 at $2 \mu\text{m}$ at the apex of the bow shock (yellow spot), based on the VLA and NTT observations, respectively. A precise alignment of these images has been made possible because a number of SiO and H_2O masers in radio wavelengths have been identified with stellar sources in the diffraction-limited $2.2\text{-}\mu\text{m}$ IR images to within 30 mas (95). The above 1950 coordinates are with respect to 17 hours, 42 min, 29 sec, $-28^\circ 59'$.

produced by pollution (mass loading) of the IRS 16 wind by the material stripped from the clump surfaces (63).

The High-Energy Emission of Sgr A East: Irradiation of Relativistic Particles by the Luminous Central Sources

The CND is a powerful source of mid- to far-IR continuum emission [luminosity, about 2×10^6 the luminosity of the sun (L_{\odot})], which is interpreted to be re-radiation by warm dust in the ring that has absorbed the same power in the UV (64, 65). This implies a total UV luminosity in the region of about $2 \times 10^7 L_{\odot}$, which is consistent with the radio continuum emission from Sgr A West and with the far-IR line emission from the ring (66). On a larger scale, there is a diffuse halo of non-thermal continuum emission with a diameter of about $7'$ to $10'$ surrounding the oval-shaped nonthermal structure Sgr A East, which itself lies close to the CND (Figs. 3 and 4). The power-law energy distribution of the relativistic electrons within the shell and the halo has a spectral index estimated to be 3 and 2.4, respectively, in these sources (38). The optical depth (defined as the size of the emitting region divided by the photon's mean free path) toward Sgr A East and the halo at low frequencies lead us to consider a mixture of both thermal and nonthermal gas in the halo, though displaced to the front side of Sgr A East. The schematic diagram in Fig. 7 assumes a geometry in which the Sgr A East shell lies close to, but behind, the Galactic center, whereas the diffuse Sgr A East halo surrounds the Galactic center and the shell.

The strong coupling between the relativistic decay particles in Sgr A East, its halo, and the external UV and IR radiation from the central 1 to 2 pc can explain the nature of the EGRET γ -ray source 3EGJ1746-2852, which is positioned at Galactic longitude $l = 0.11^\circ$ and

Galactic latitude $b = -0.04^\circ$ (67–69). The inverse Compton (x-ray and γ -ray) emissivity produced by this relativistic e^+e^- population bathed by the IR and UV radiation is emitted isotropically from within a volume $V \sim 250 \text{ pc}^3$ in Sgr A East, corresponding to a shell with radius $R \gg 5 \text{ pc}$ and thickness $\Delta R \gg 1 \text{ pc}$. The remaining continuum component of importance is bremsstrahlung emission resulting from the interaction between the relativistic leptons and the ambient nuclei. In this model, the primary physical interaction accounting for the broadband spectrum of Sgr A East (Fig. 8) is the shock wave acceleration of protons to relativistic energies (61) due to the collision of Sgr A East and its nearby molecular clouds. As these highly energetic particles escape from the shock wave regions, they scatter with the ambient (low-energy) protons, which produces a proliferation of neutral and charged pions. The neutral pions decay and form a γ -ray spectrum, whereas the charged pions decay into muons and thence into electrons and positrons. In this model, the overall spectrum from Sgr A East is a superposition of the γ -rays from π^0 decays, synchrotron radiation by the relativistic leptons produced during the decay of the charged pions, bremsstrahlung emission by these electrons and positrons, and their Comptonization (the process by which energetic particles boost the energy of the ambient radiation through scattering events) of the IR and UV radiation from the central 1 to 2 pc.

Interaction of Sgr A East and the 50 km s^{-1} Molecular Cloud

The relationship between the dense gas clouds in the inner 10 to 20 pc of the Galaxy and the CND, Sgr A*, and Sgr A East is central to our understanding of the current environment and recent history of the Galactic center. In the past few years it has become apparent that Sgr A East, although lying almost entirely behind the

center, is close enough to partially envelop Sgr A West, and the high pressure associated with this remnant is sufficient to disturb the nearby 50 km s^{-1} cloud (70) and quite possibly the CND as described below.

The initial evidence for this interaction with the 50 km s^{-1} cloud came from observations of the cloud in CO and millimeter wavelength emission from cold dust, which showed how the atomic and molecular gas curved around the nonthermal shell as if in response to an interaction (70–74). Further molecular line observations demonstrated a velocity gradient consistent with acceleration by Sgr A East (75). More recent studies at higher resolution with the ammonia molecule (76) have confirmed these ideas and suggest that the gas is warmer as a result of this disturbance. Supporting evidence has also been provided by the detection of OH masers at 1720 MHz associated with Sgr A East (36, 77). Empirically, these masers occur in the Galaxy where supernova remnants strike adjacent molecular clouds (78). There are theoretical reasons for this: When the density and temperature in the gas fall within a restricted range ($n \sim 10^5 \text{ cm}^{-3}$, $T \sim 50$ to 125 K), collisions of H_2 molecules will invert the 1720-MHz transition of the OH molecule (79, 80). The production of a significant abundance of OH in the post-shock wave gas requires the dissociation of water. This can be achieved by UV irradiation of the molecular gas, but if this is too intense, the resultant grain heating generates a far-IR continuum that inverts the 1665- and 1667-MHz transitions instead (80). On the other hand, dissociation can occur because of the irradiation of the molecular cloud by x-rays produced by the hot gas in the interior of the adjacent supernova remnant (SNR) (Fig. 9). These conditions, and an adequate abundance of OH, can be achieved in shock waves in molecular clouds (81), and in Sgr A East the conditions agree with this model (72). Emission in IR rotational-vibration transitions from hot molecular hydrogen has been observed toward the masers in Sgr A East (77) (Fig. 10), although further observations are required to confirm that the emission comes from gas that has been heated by a shock wave rather than (for example) by irradiation from nearby hot stars.

Interaction of Sgr A East with the CND

The suggestion that the front edge of the expanding shell may also have overrun the CND (39) is more indirect than the case of an interaction of Sgr A East with the 50 km s^{-1} molecular cloud, as it is harder to detect the associated velocity gradients because of the clumpy and disordered nature of the CND. The evidence suggests that the CND is disturbed from outside, probably by Sgr A East. First, although the ionized gas associated with Sgr A West is absorbing most of the nonthermal emission from Sgr A East and

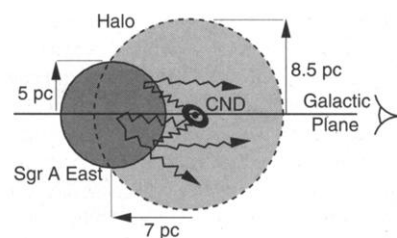
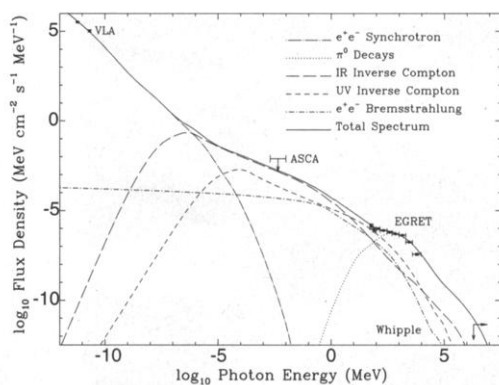


Fig. 7 (left). Schematic diagram showing the relative positions and sizes of the halo and Sgr A East relative to Sgr A*, which is shown here as a point centered within the CND. The thermal three-arm spiral radio source Sgr A West is also contained within the CND. Low-energy photons arising from the CND are shown to be upscattered to higher energies by relativistic particles from Sgr A East. **Fig. 8 (right).** The broadband spectrum calculated self-consistently using the particle decay products from proton-proton scattering. The electron and positron distributions result from the decay of pions produced in these scattering events. The data included in this plot are from (38, 89, 96, 97). ASCA, Advanced Satellite for Cosmology and Astrophysics; EGRET, Energetic Gamma Ray Experiment Telescope; Whipple, the Whipple Observatory gamma-ray telescope.



must therefore lie in front, there is still non-thermal emission present at $\lambda = 90$ cm toward thermally ionized gas; Sgr A West is therefore embedded within Sgr A East but lies toward the frontmost edge. Second, near-IR observations have revealed a linear filament of H_2 emission located at the western edge of the CND running parallel to the nonthermal shell of Sgr A East. The sheetlike morphology association with OH maser source C at 1720 MHz (Fig. 10; see also Web fig. 1 at www.sciencemag.org/feature/data/1046905.shl), and the lack of evidence for UV heating in the form of thermal radio continuum or Br γ emission, imply that this filament is shock-heated. The high velocity of the sheetlike H_2 gas and the OH maser C are consistent with a model in which they outline the outer envelope of the CND, probably shock-excited externally by the nonther-

mal source Sgr A East (Fig. 10). Almost all members of the class of OH masers observed at 1720 MHz are associated with nonthermal radio continuum sources. It is possible that the shocked gas is associated with the 50 km s^{-1} cloud and happens to be aligned fortuitously along the outer edge of the CND, but the morphology in several tracers appears to link it to the CND (39). Finally, highly negative radial velocity H_2CO , OH, HI, and HCO^+ absorption features, with velocities of about -190 km s^{-1} (82–86) have been observed toward Sgr A West. The kinematic and spatial distribution of this gas place it at the Galactic center [but see (87) for an alternative interpretation]. If this gas is associated with Sgr A West, the only plausible explanation for its highly negative velocity is that it has been accelerated by Sgr A East.

Sgr A East: Is this Remnant the Result of an Interaction Between a Star and the Black Hole?

The ample evidence that the nonthermal shell of Sgr A East is physically interacting with the 50 km s^{-1} molecular cloud has suggested a model in which an explosion occurred inside the molecular cloud and created the Sgr A East shell (37, 71, 74). In this scenario, the mass ($6 \times 10^4 M_\odot$) of neutral gas that curves around the shell of Sgr A East has been swept up by the explosion (74). Although resembling a SNR, Sgr A East's inferred energetics ($\sim 4 \times 10^{52}$ ergs) (74) appear to be extreme and have generated some uncertainty regarding this interpretation. The explosion that produced Sgr A East may instead have been the tidal disruption of a main sequence star whose trajectory took it within 10 Schwarzschild radii of the central object (88). In this scenario, the gravitational field of the black hole squeezes the star into a long thin spike during its inward trajectory, and the work done by gravity is dissipated quickly into the internal energy of the unfortunate intruder. The energy stored in this fashion can exceed the binding energy of the star by several orders of magnitude, and so when it recedes from its location of closest approach to the black hole, the star expands explosively, very much like a supernova shell, except with a much greater energy. Alternatively, the energetic requirements are significantly reduced if the explosion that created Sgr A East expanded into a preexisting cavity rather than a dense cloud. The energy required is about the thermal energy of the $T \sim 10 \text{ keV}$, $n_e \sim 6 \text{ cm}^{-3}$ gas detected in x-rays (Fig. 9) by the Advanced Satellite for Cosmology and Astrophysics (89), about 5×10^{51} erg, which is equivalent to several normal supernovae.

The formation of such a cavity in the original 50 km s^{-1} cloud can be described as follows. The distribution of molecular emission in CO, H_2CO , CS, and HCO^+ indicates a lack of molecular gas at velocities around 50 to 60 km s^{-1} toward Sgr A West (90–92). This suggests a scenario in which both the cavity and the CND are a consequence of the dynamical interaction of the original 50 km s^{-1} cloud and the gravitational potential of the inner few parsecs of the Galaxy. In this model, star formation has been taking place in the initial 50 km s^{-1} molecular cloud as it sweeps through the Galactic center, engulfing Sgr A*. The inner regions of the cloud are deflected, effecting a collision between gaseous material that passes on either side of Sgr A* with opposite angular momenta. The resulting dissipation permits this gas to become bound to the Galactic center. The subsequent circularization and settling happens rapidly (93). This model is consistent with the asymmetry and disorder of the CND, which indicate that it is perhaps a few tens of orbits old (94). Meanwhile, the outer part of the 50 km s^{-1} molecular cloud continues passing through the Galactic center on its way to its present position be-

Fig. 9. The brightest region of continuum emission from Sgr A East at $\lambda = 20$ cm with a resolution of 3.1×1.5 arc sec is shown in blue; the bright white spot coincident with Sgr A* is superimposed on the brightest portion of diffuse x-ray emission from the Galactic center, shown in red (89). The bright red spot in the southwest corner is associated with a low-mass eclipsing x-ray binary system (98). The crosses represent the positions of OH masers at 1720 MHz, signifying the region where a molecular cloud is interacting with the nonthermal shell of Sgr A East (36).

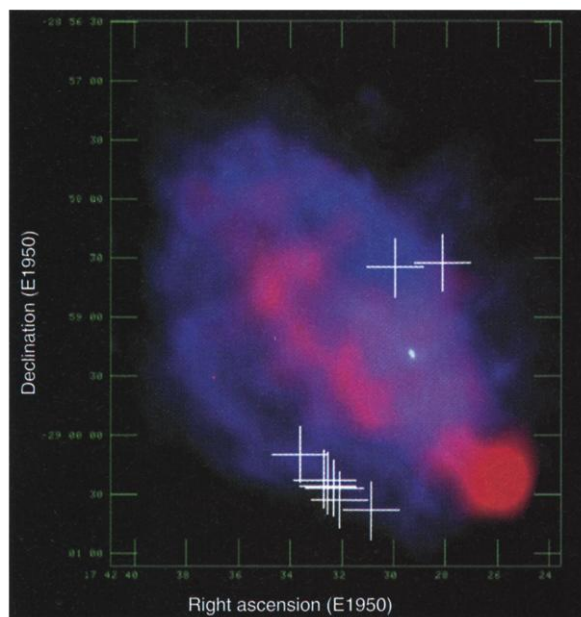
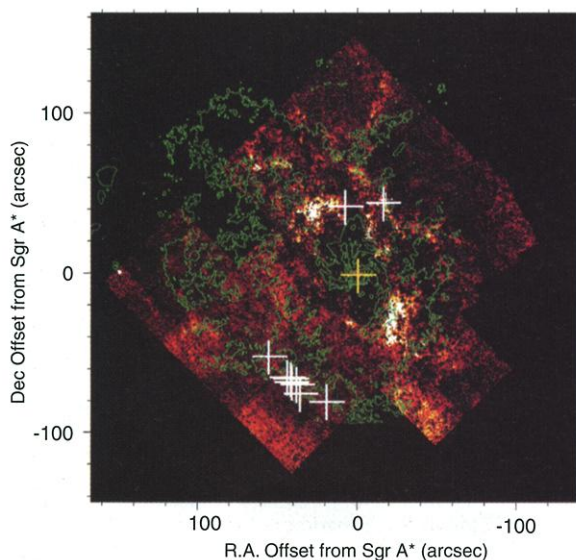


Fig. 10. Contours of radio continuum emission at 6 cm (green) as seen in Fig. 4 are superimposed on the distribution of H_2 emission using the Hubble Space Telescope near-IR camera and multiobject spectrometer. The white crosses indicate OH (1720 MHz) maser positions, whereas the yellow cross coincides with Sgr A*. The two crosses toward the top left and top right are masers B and C lying on the CND and the H_2 filament at 134 and 43 km s^{-1} , respectively. The contours of Sgr A West lie within the brightest H_2 -emitting features, delineating the CND (39). Dec, declination; R.A., right ascension. See Web fig. 1 at www.sciencemag.org/feature/data/1046905.shl.



tween 5 and 30 pc behind Sgr A West. The interaction would have occurred $\sim 3 \times 10^5$ years ago, and during this time, the progenitor of Sgr A East could have exploded inside the cavity that has been cleared out by the transit through the Galactic center.

Summary

This review has examined the common thread of interaction among five sources in order to explain the various observed phenomena in the rich, complex, and unique center of the Galaxy. Any self-consistent picture of this region must include an accounting of how the five principal members of this closely packed system interact physically with each other. The constituents discussed are the black hole Sgr A* (a name derived from its identification at radio wavelengths); the surrounding cluster of bright stars IRS 16; the red supergiant star IRS 7, with its attached cometary-like tail; the CND of molecular gas; and a powerful supernovallike remnant known as Sgr A East, which envelops many of the other objects. In spite of the fact that the Galactic center is totally obscured at optical wavelengths, the precision with which the mass of the black hole was determined is creating new puzzles in understanding the type of activity found in nuclei of galaxies that are not obscured at optical wavelengths; in particular, why this massive black hole has such an unexpectedly low radiative efficiency. Understanding the answer to this puzzle will greatly improve our overall view of how the central engines (also thought to be massive black holes) in active galactic nuclei derive their power and characteristics.

References and Notes

- B. Balick and R. Brown, *Astrophys. J.* **194**, 265 (1974).
- M. T. McGinn, K. Sellgren, E. E. Becklin, D. N. B. Hall, *Astrophys. J.* **338**, 824 (1989).
- G. H. Rieke and M. J. Rieke, *Astrophys. J.* **344**, L5 (1989).
- K. Sellgren, M. T. McGinn, E. E. Becklin, D. N. B. Hall, *Astrophys. J.* **359**, 112 (1990).
- J. Haller et al., *Astrophys. J.* **456**, 194 (1996).
- R. Genzel, N. Thatte, A. Krabbe, H. Kroker, L. E. Tacconi-Garman, *Astrophys. J.* **472**, 153 (1996).
- A. Eckart and R. Genzel, *Nature* **383**, 415 (1996).
- , *Mon. Not. R. Astron. Soc.* **284**, 576 (1997).
- A. Ghez, B. L. Klein, M. Morris, E. E. Becklin, *Astrophys. J.* **509**, 678 (1998).
- R. Genzel and A. Eckart, in *The Central Parsec of the Galaxy* [Astronomical Society of the Pacific (ASP) Conference Series, ASP, San Francisco, CA, 1999], vol. 186, pp. 3–17.
- A. Ghez, M. Morris, E. E. Becklin, in *The Central Parsec of the Galaxy* (ASP Conference Series, ASP, San Francisco, CA, 1999), vol. 186, pp. 18–23.
- M. Myoshi et al., *Nature* **374**, 623 (1995).
- D. Lynden-Bell M. J. and Rees, *Mon. Not. R. Astron. Soc.* **152**, 461 (1971).
- D. C. Backer and R. A. Sramek, *Astrophys. J.* **524**, 805 (1999).
- M. J. Reid, A. C. S. Readhead, R. C. Vermulen, R. N. Treuhaft, *Astrophys. J.* **524**, 816 (1999).
- G. C. Bower and D. C. Backer, in *The Central Parsec of the Galaxy* (ASP Conference Series, ASP, San Francisco, CA, 1999), vol. 186, pp. 80–88.
- E. Maoz, *Astrophys. J.* **494**, L181 (1998).
- R. Antonucci, *Annu. Rev. Astron. Astrophys.* **31**, 473 (1993).
- R. Güsten et al., *Astrophys. J.* **318**, 124 (1987).
- M. C. H. Wright, R. Genzel, R. Güsten, D. T. Jaffe, in *The Galactic Center*, D. C. Backer, Ed. (American Institute of Physics, New York, 1987), pp. 133–137.
- J. M. Jackson et al., *J. Astrophys. J.* **402**, 173 (1993).
- A. Krabbe, R. Genzel, S. Drapatz, V. Rotaciuc, *Astrophys. J.* **382**, L19 (1991).
- D. N. C. Hall, S. G. Kleinmann, N. Z. Scoville, *Astrophys. J.* **260**, L63 (1982).
- T. R. Geballe, R. Wade, K. Krisciunas, I. Gatley, M. C. Bird, *Astrophys. J.* **320**, 562 (1987).
- D. A. Allen, A. R. Hyland, D. J. Hillier, *Mon. Not. R. Astron. Soc.* **244**, 706 (1990).
- E. R. Wollman, T. R. Geballe, J. H. Lacy, C. H. Townes, D. M. Rank, *Astrophys. J.* **218**, L103 (1977).
- J. H. Lacy, F. Baas, C. H. Townes, T. R. Geballe, *Astrophys. J.* **227**, 17L (1979).
- E. Serabyn, J. H. Lacy, C. H. Townes, R. Bharat, *Astrophys. J.* **326**, 171 (1988).
- U. J. Schwarz, J. D. Bregman, J. H. van Gorkom, *Astron. Astrophys. J.* **215**, 33 (1989).
- T. M. Herbst, S. V. W. Beckwith, M. Shure, *Astrophys. J.* **411**, L21 (1993).
- D. Roberts and W. M. Goss, *Astrophys. J.* **86**, 133 (1993).
- F. Yusef-Zadeh, M. Morris, R. Ekers, in *The Center of the Galaxy*, International Astronomical Union (IAU) Symposium No. 136, M. Morris, Ed. (Kluwer, Dordrecht, Netherlands, 1989), pp. 443–451.
- D. Roberts, F. Yusef-Zadeh, M. Goss, *Astrophys. J.* **459**, 627 (1996).
- F. Yusef-Zadeh, D. A. Roberts, J. Biretta, *Astrophys. J.* **499**, L159 (1998).
- J.-H. Zhao and W. M. Goss, *Astrophys. J.* **499**, L163 (1998).
- F. Yusef-Zadeh, D. A. Roberts, W. M. Goss, D. Frail, A. Green, *Astrophys. J.* **466**, L25 (1996).
- F. Yusef-Zadeh and M. Morris, *Astrophys. J.* **320**, 545 (1987).
- A. Pedlar et al., *Astrophys. J.* **342**, 769 (1989).
- F. Yusef-Zadeh et al., in *The Central Parsec of the Galaxy* (ASP Conference Series, ASP, San Francisco, CA, 1999), vol. 186, pp. 197–213.
- F. Melia, *Astrophys. J.* **426**, 577 (1994).
- F. Melia and R. Coker, in *The Central Parsec of the Galaxy* (ASP Conference Series, ASP, San Francisco, CA, 1999), vol. 186, pp. 214–223.
- R. Coker and F. Melia, *Astrophys. J.* **488**, L149 (1997).
- T. Beckert and W. J. Duschl, *Astron. Astrophys.* **328**, 95 (1997).
- H. Falcke, K. Mannheim, P. L. Biermann, *Astron. Astrophys.* **278**, 1 (1993).
- R. Narayan, I. Yi, R. Mahadevan, *Nature* **374**, 623 (1995).
- R. Narayan, R. Mahadevan, J. Grindley, R. G. Popham, C. Gammie, *Astrophys. J.* **492**, 554 (1997).
- V. Kowalenko and F. Melia, *Mon. Not. R. Astron. Soc.*, in press.
- F. Yusef-Zadeh, M. Morris, R. D. Ekers, *Nature* **348**, 45 (1990).
- M. Wardle and F. Yusef-Zadeh, *Nature* **357**, 308 (1992).
- J. H. Zhao, W. M. Goss, K. Y. Lo, R. D. Ekers, *Nature* **354**, 46 (1991).
- F. Melia, R. Coker, F. Yusef-Zadeh, *Astrophys. J.* **460**, L33 (1996).
- D. Lutz, A. Krabbe, R. Genzel, *Astrophys. J.* **418**, 244 (1993).
- M. J. Lebofsky, G. H. Rieke, A. T. Tokunaga, *Astrophys. J.* **263**, 736 (1982).
- K. Sellgren, D. N. B. Hall, S. G. Kleinmann, N. Z. Scoville, *Astrophys. J.* **317**, 881 (1987).
- F. Yusef-Zadeh and M. Morris, *Astrophys. J.* **371**, L59 (1991).
- E. Serabyn, J. H. Lacy, J. M. Achtermann, *Astrophys. J.* **378**, 557 (1991).
- A. S. Cotera et al., in *The Central Parsec of the Galaxy* (ASP Conference Series, ASP, San Francisco, CA, 1999), vol. 186, pp. 240–249.
- F. Yusef-Zadeh and F. Melia, *Astrophys. J.* **385**, L41 (1992).
- J. H. Lacy, J. M. Achtermann, E. Serabyn, *Astrophys. J.* **380**, L71 (1991).
- R. D. Ekers, J. H. van Gorkom, U. J. Schwartz, W. M. Goss, *Astron. Astrophys.* **122**, 143 (1983).
- P. G. Mezger and J. E. Wink, *Astron. Astrophys.* **157**, 252 (1986).
- J. E. Dyson, T. W. Hartquist, S. Biro, *Mon. Not. R. Astron. Soc.* **261**, 430 (1993).
- J. E. Dyson and T. W. Hartquist, *Mon. Not. R. Astron. Soc.* **269**, 1117 (1994).
- E. E. Becklin, I. Gatley, M. W. Werner, *Astrophys. J.* **258**, 135B (1982).
- J. A. Davidson et al., *Astrophys. J.* **387**, 189 (1992).
- R. Genzel, D. M. Watson, M. K. Crawford, C. H. Townes, *Astrophys. J.* **297**, 766 (1985).
- R. C. Hartman et al. *Astrophys. J.* **79**, 202 (1999).
- F. Melia, F. Yusef-Zadeh, M. Fatuzzo, *Astrophys. J.* **508**, 676 (1998a).
- F. Melia, M. Fatuzzo, F. Yusef-Zadeh, S. Markoff, *Astrophys. J.* **508**, L65 (1998b).
- A. Sandqvist, *Astron. Astrophys.* **33**, 413 (1974).
- P. G. Mezger et al., *Astron. Astrophys.* **209**, 337 (1989).
- M. Wardle, F. Yusef-Zadeh, T. R. Geballe, in *The Central Parsec of the Galaxy* (ASP Conference Series, ASP, San Francisco, CA, 1999), vol. 186, pp. 432–440.
- J. Lasenby, F. Yusef-Zadeh, A. Lasenby, in *The Center of the Galaxy*, IAU Symposium No. 136, M. Morris, Ed. (Kluwer, Dordrecht, Netherlands, 1989), pp. 365–370.
- R. Zylka, P. G. Mezger, J. E. Wink, *Astron. Astrophys.* **234**, 133 (1990).
- E. Serabyn, J. H. Lacy, J. M. Achtermann, *Astrophys. J.* **395**, 166 (1992).
- A. Coil and P. T. P. Ho, *Astrophys. J.* **513**, 752 (1999).
- F. Yusef-Zadeh, D. A. Roberts, W. M. Goss, D. Frail, A. Green, *Astrophys. J.* **512**, 230 (1999).
- D. A. Frail, M. W. Goss, V. I. Slysh, *Astrophys. J.* **424**, L111 (1994).
- M. Elitzur, *Astrophys. J.* **203**, 124 (1976).
- P. Lockett, E. Gauthier, M. Elitzur, *Astrophys. J.* **511**, 235 (1999).
- M. Wardle, *Astrophys. J.* **525**, L101 (1999).
- J. M. Marr, A. L. Rudolph, T. A. Pauls, M. C. Wright, D. C. Backer, *Astrophys. J.* **400**, L29 (1992).
- T. Pauls, K. J. Johnston, T. L. Wilson, J. M. Marr, A. Rudolph, *Astrophys. J.* **403**, L13 (1993).
- F. Yusef-Zadeh, A. Lasenby, J. Marshall, *Astrophys. J.* **410**, L27 (1993).
- F. Yusef-Zadeh, J. H. Zhao, W. M. Goss, *Astrophys. J.* **442**, 646 (1995).
- J. H. Zhao, W. M. Goss, P. T. P. Ho, *Astrophys. J.* **450**, 122 (1995).
- H. S. Liszt and W. B. Burton, *Astrophys. J.* **98**, 679 (1995).
- A. Khokhlov and F. Melia, *Astrophys. J.* **457**, L61 (1996).
- K. Koyama et al., *Pub. Astron. Soc. Jpn.* **48**, 249 (1996).
- A. Sandqvist, A. Wootten, R. B. Loren, *Astron. Astrophys.* **152**, 25 (1985).
- A. Sandqvist, *Astron. Astrophys.* **223**, 293 (1989).
- E. Serabyn, R. Güsten, J. E. Walmsley, J. E. Wink, R. Zylka, *Astron. Astrophys.* **169**, 85 (1986).
- R. H. Sanders, *Mon. Not. R. Astron. Soc.* **294**, 35 (1998).
- M. Morris and E. Serabyn, *Annu. Rev. Astron. Astrophys.* **34**, 645 (1996).
- K. M. Menten, M. J. Reid, A. Eckart, R. Genzel, *Astrophys. J.* **475**, L111 (1997).
- H. A. Mayer-Hasselwander et al., *Astron. Astrophys.* **335**, 161 (1998).
- J. H. Buckley et al., in *Proceedings of the 25th International Cosmic Ray Conference (Durban, South Africa)*, M. A. Potgieter, C. Raubenheimer, D. J. van der Walt, Eds. (Potchetstrom, Durban, South Africa, 1997), vol. 3, pp. 233–236.
- Y. Maeda, K. Koyama, M. Sakano, Y. Takeshima, S. Yamauchi, *Pub. Astron. Soc. Jpn.* **48**, 417 (1996).
- We thank A. Eckart, A. Ghez, D. Roberts, and S. Stolovy for their help in providing figures used here. This research was partially supported by NASA.